

Supplementary Information for

Rational design of a functionalized metal-organic framework for ratiometric fluorimetric sensing Hg²⁺ in environmental water

Yanli Li ^{a,b}, Yanmei Si ^{a*}, Genmei Yang ^b, Lixia Yang ^b, Hua Wang ^c

^a College of Forensic Medicine and Laboratory Medicine, Jining Medical University, Jining 272067, PR China.

^b College of Environmental and Chemical Engineering, Nanchang Hangkong University, Nanchang 330063, PR China.

^c School of Life Science, Huzhou University, Huzhou, 313000, PR China.

*Corresponding authors : siyanmei90@126.com

Table of Content

Fig. S1. Size distribution of Eu-MOF/BA.

Fig. S2. Infrared spectra of DCPB and Eu-MOF/BA.

Fig. S3. UV-vis spectra of Eu^{3+} , DCPB, Eu-MOF/BA.

Fig. S4. Images of Eu-MOF/BA in the solution of different pH under the UV lamp at 265 nm.

Fig. S5. Images of Eu-MOF/BA in the solution containing various interferents under UV lamp at 265 nm.

Fig. S6. ^1H NMR spectra of (A) PBA, (B) PBA+ Hg^{2+} , (C) phenylmercury chloride.

Fig. S7. ^{13}C NMR spectra of (A) PBA+ Hg^{2+} , (B) phenylmercury chloride.

Table S1. Comparison of the detection performance among different methods for Hg^{2+} assay.

Characterization

Scanning electron microscope (SEM, Hitachi-SU1510) and transmission electron microscope (TEM, FEI Talos F200X) were used to characterize the structural and morphological information of Eu-MOF/BA. X-ray diffraction (XRD) patterns were carried out with an X-ray diffractometer (Bruker, D8 Advance, Germany) with Cu K α radiation ($\lambda=1.542\text{\AA}$). The Fourier transform spectra (FT-IR) were measured using in situ diffuse reflectance infrared Fourier transform spectroscopy (Nicolet IS50, Thermo fisher). The thermogravimetric analysis (TGA) was conducted on the Mettler Toledo TGA / DSC-1 system. UV-Vis-IR spectra were recorded by spectrophotometer (UV-3600 plus). Fluorescence spectra were collected using a fluorescence spectrometer (Hitachi, F4500) under a 270 nm excitation. Parameter setting: scanning speed of 240 nm/min, excitation and emission slit of 5 nm, the voltage of 950 V.

Additional figures

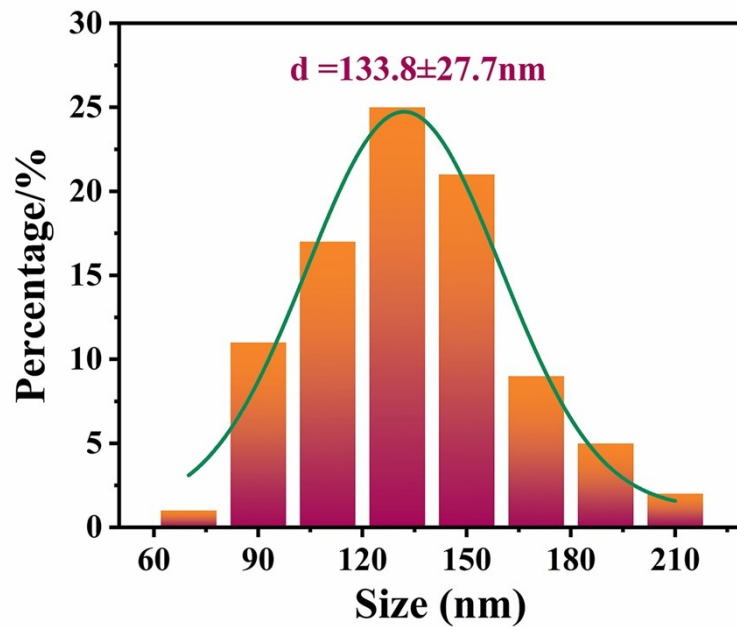


Fig.S1. Size distribution of Eu-MOF/BA.

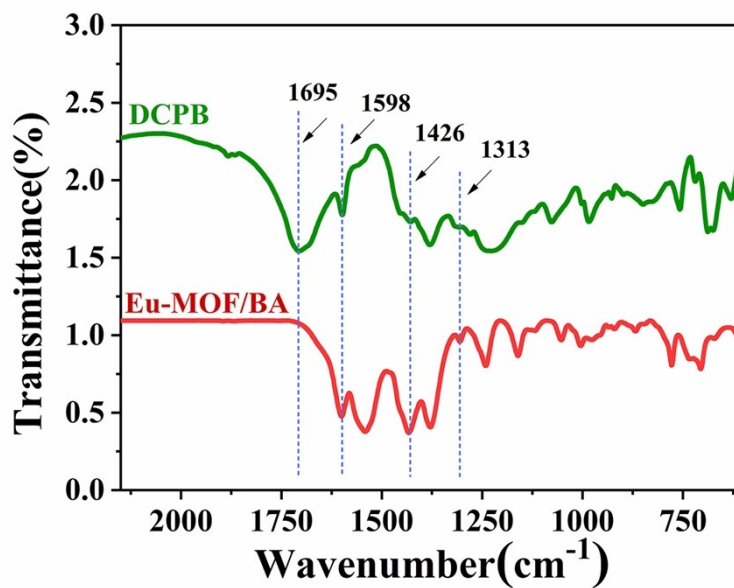


Fig.S2. Infrared spectra of DCPB and Eu-MOF/BA.

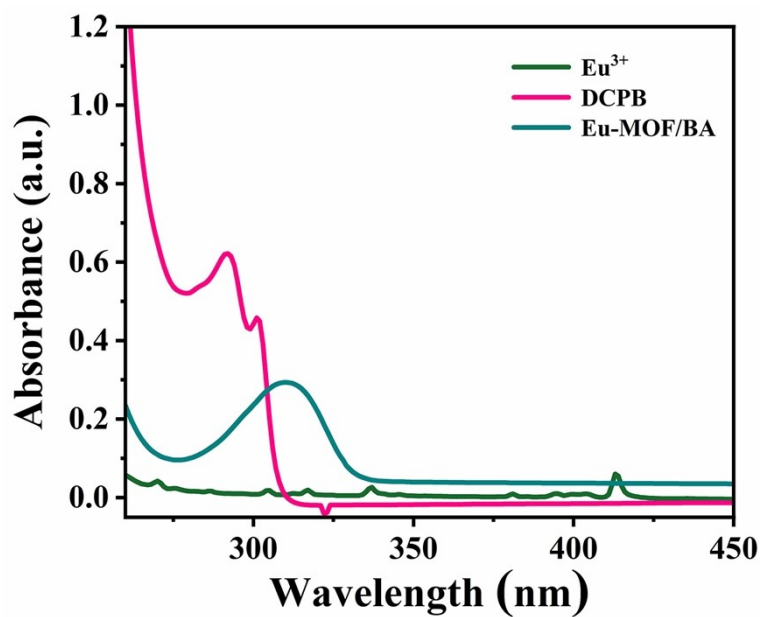


Fig.S3. UV-vis spectra of Eu^{3+} , DCPB, Eu-MOF/BA.



Fig.S4. Images of Eu-MOF/BA in the solution of different pH under the UV lamp at 265 nm.

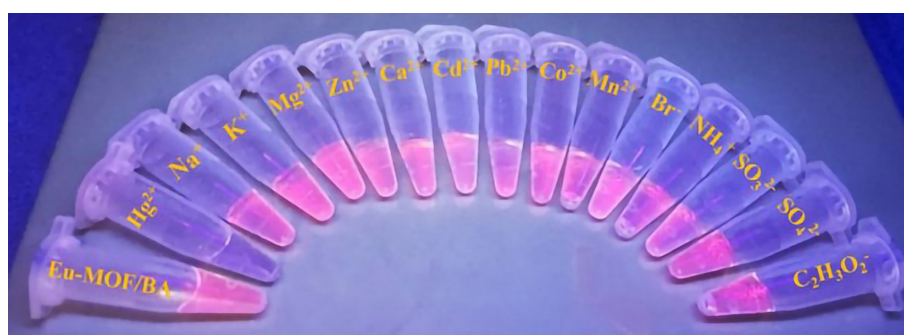
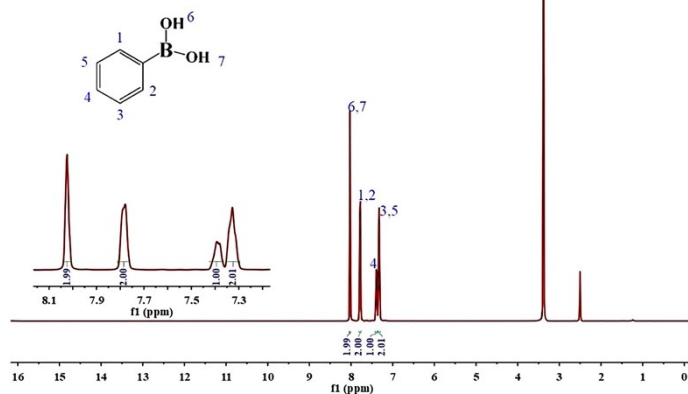


Fig.S5. Images of Eu-MOF/BA in the solution containing various interferents under UV lamp at 265 nm.

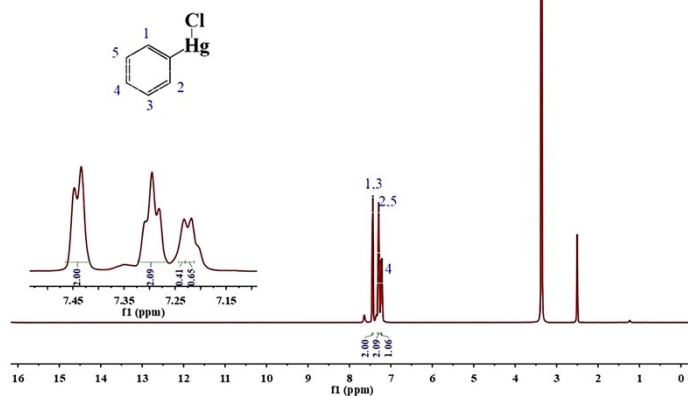
(A) ^1H NMR spectra of PBA

^1H NMR (DMSO- d_6 , 500 MHz) δ (ppm) 8.03 (s, 2H), 7.79 (d, $J = 7.5$ Hz, 2H), 7.40-7.38(m, 1H), 7.34-7.31(m, 2H)



(B) ^1H NMR spectra of PBA+ Hg^{2+}

^1H NMR (DMSO- d_6 , 500 MHz) δ (ppm) 7.44 (d, $J = 7$ Hz, 2H), 7.30 (t, $J = 7.5$ Hz, 2H), 7.23 (t, $J = 7.5$ Hz, 1H)



(C) ^1H NMR spectra of phenylmercury chlorid

^1H NMR (DMSO- d_6 , 500 MHz) δ (ppm) 7.44 (d, $J = 7.5$ Hz, 2H), 7.29 (t, $J = 8.0$ Hz, 2H), 7.22 (t, $J = 7.5$ Hz, 1H)

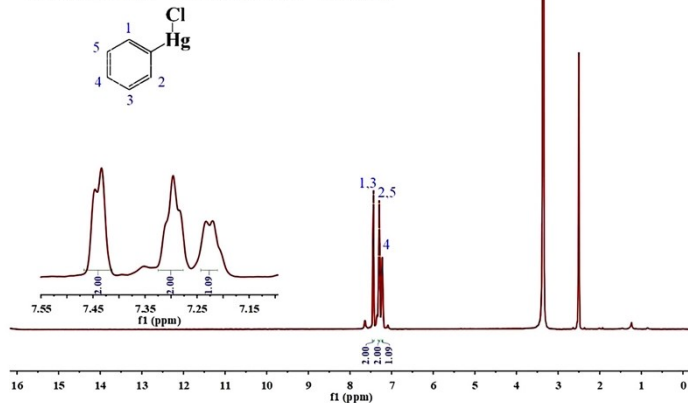


Fig. S6. ^1H NMR spectra of (A) PBA, (B) PBA+ Hg^{2+} , (C) phenylmercury chloride.

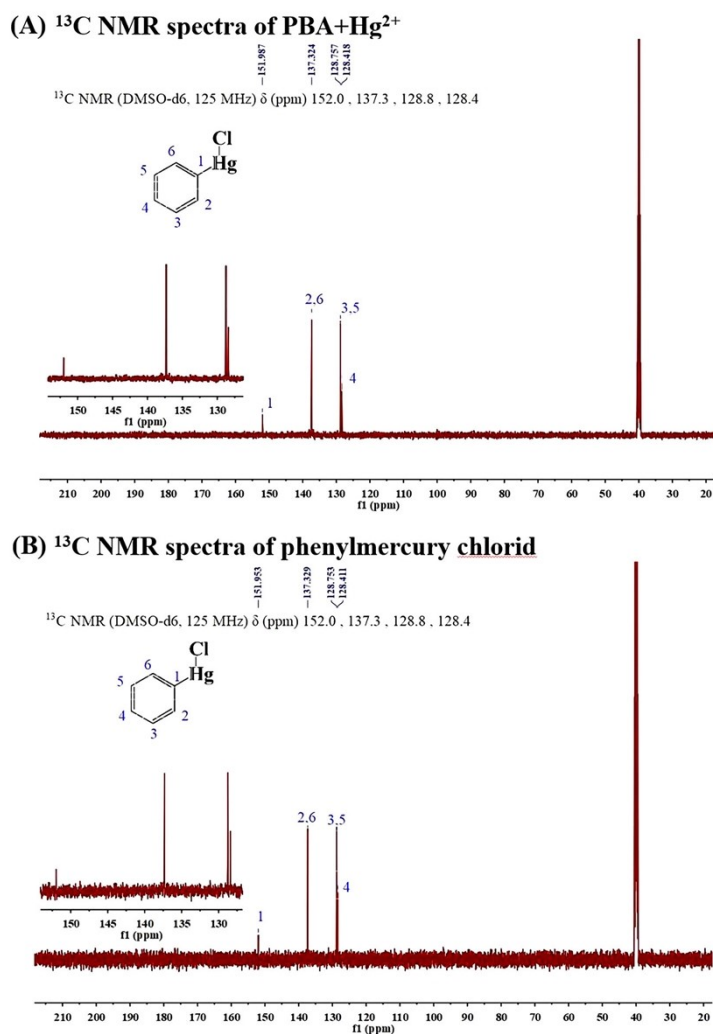


Fig. S7. ^{13}C NMR spectra of (A) PBA+Hg $^{2+}$, (B) phenylmercury chloride.

Table S1. Comparison of the detection performance among different methods for Hg $^{2+}$ assay.

Methods	Linear range (μM)	LOD (nM)	Refs
Electrochemical	0.5-50	2	[1]
SERS	0.005-0.5	0.5	[2]
Colorimetric	0.085-4.7	5.88	[3]
Fluorescent	0.1-50	1.6	[4]
Fluorescent	0.01-1	3.65	[5]
Fluorescent	0.0005-50	0.5	[6]
This work	0-50.0	0.0890	-

Reference

- [1] J. Zhang, X. Xu, L. Chen, An ultrasensitive electrochemical bisphenol A sensor based on hierarchical Ce-metal-organic framework modified with cetyltrimethylammonium bromide, *Sensor. and Actuat. B-Chem.*, 2018, **261**, 425-433.
- [2] S. Ali, M. Mansha, N. Baig, S. A. Khan, Recent trends and future perspectives of emergent analytical techniques for mercury sensing in aquatic environments, *Chem. Rec.*, 2022, **22**, 202100327.
- [3] M. U. Gürbüz, E. Gökhan A. S. Ertürk, Tren-cored PAMAM dendrimer/silver nanocomposites: efficient colorimetric sensors for the determination of mercury ions from aqueous solutions, *Chemistry Select.*, 2019, **4**, 7715-7721.
- [4] Q. Xu, R. G. Su, Y. S. Chen, S. T. Sreenivasan, N. Li, X. S. Zheng, J. F. Zhu, H. B. Pan, W. J. Li, C. M. Xu, Z. H. Xia, L. M. Da, Metal charge transfer doped carbon dots with reversibly switchable, ultra-high quantum yield photoluminescence, *ACS. Appl. Nano. Mater.*, 2018, **1**, 1886-1893.
- [5] S. O. Tümay, V. Şanko, A. Şenocak, E. Demirbas, A hybrid nanosensor based on novel fluorescent iron oxide nanoparticles for highly selective determination of Hg²⁺ ions in environmental samples, *New. J. Chem.*, 2021, **45**, 14495-14507.
- [6] S. C. G. Kiruba Daniel, A. Kumar, K. Sivasakthi, C. S. Thakur, Handheld, low-cost electronic device for rapid, real-time fluorescence-based detection of Hg²⁺, using aptamer-templated ZnO quantum dots, *Sensor. and Actuat. B-Chem.*, 2019, **290**, 73-78.